The Orientation of CO in Heme Proteins Determined by Time-Resolved Mid-IR Spectroscopy: Anisotropy Correction for Finite Photolysis of an Optically Thick Sample

Manho Lim

Department of Chemistry and CIMS (POSTECH), Pusan National University, Busan 609-735, Korea
Received March 6, 2002

A systematic way of determining the equilibrium orientation of carbon monoxide (CO) in heme proteins using time-resolved polarized mid-IR spectroscopy is presented. The polarization anisotropy at pump-probe delay time of zero in the limit of zero photolysis and the angular distribution function of CO are required to obtain the equilibrium orientation of CO. An approach is developed for determining the polarization anisotropy in the zero-photolysis limit from the anisotropy measured under finite photolysis conditions in an optically thick sample where the fraction of molecules photolyzed decreases as the pump pulse passes through and is absorbed by the sample. This approach is verified by measuring the polarization anisotropy of CO of carbonmonoxy myoglobin at various levels of photolysis. This method can be readily applied to other photoselection experiments determining precise angle between transition dipoles.

Keywords : Heme protein, Optically thick sample, Time-resolved IR spectroscopy, Anisotropy.

Introduction

Myoglobin (Mb), a heme protein that reversibly binds small ligands such as O_2 and CO, has long served as a model system for understanding how the structure of a protein affects its function.[1] The active binding site in Mb, an iron(II)-containing porphyrin (heme), is embedded within the hydrophobic interior of the protein. It is known that the highly conserved amino acid residues surrounding the heme in Mb modulates its ligand binding affinity. For example, the binding affinity for CO compared to O_2 is reduced *ca.* 50 times relative to that of free heme in solution.[2,3] This discrimination is biologically important considering that only about 1% of the Mb in nonsmokers is poisoned by CO, a toxic ligand produced endogenously by catabolism of heme itself.[4]

A structural basis for discrimination against CO was suggested based on the crystal structures of MbCO which seemed to indicate that the protein forces CO to bind in a bent Fe-C-O geometry.[5] It was found that CO binds to model hemes with a linear Fe-C-O geometry[6] but binds to Mb in a bent geometry,[5] and that O_2 binds to model hemes[7-9] and Mb with a similar bent Fe-O-O geometry.[10] Considering that the O_2 prefers to bind to the heme in a bent geometry, which is unaffected by the Mb, it was presumed that the protein forces CO to bind in a bent geometry, thereby reducing the affinity of the heme in Mb for CO relative to O_2.[2-11] This mechanism seemed so compelling that it became a classic example of the relation between protein structure and function.[12] However, the premise that Fe-C-O moiety in Mb is forced to be bent and that bending is functionally relevant in MbCO[13,14] remains controversial. The orientation of CO in MbCO determined using x-ray diffraction with various crystals as well as a variety of spectroscopic techniques, reveals

inconsistencies.[1,15-17] Regardless of the origin of variations in the reported orientation, the need for an unambiguously accurate structure determination under physiologically relevant conditions is evident.

The method of photoselection[18,19] combined with polarized IR spectroscopy[15,20-29] has been used to determine the orientation of CO relative to the heme plane normal in Mb. Earlier polarized IR measurements on various heme proteins at ambient temperature[21-23,25,26,28,29] reported that the orientation of CO in heme protein is bent at different angles ranging from 15° to 35°, similar to earlier crystal structure.[5] However, using the same polarized IR spectroscopy, we have recently found that CO in Mb is almost linear, bent less than 7° relative to the heme plane normal,[15] consistent with more recent higher resolution X-ray crystal structure[16] and spectroscopic data in solution,[30] thereby establishing necessity of newer paradigm for how Mb discriminate against CO. Even though the theory for determining angles with photoselection spectroscopy is rigorous, there are numerous experimental pitfalls. Here we report a systematic way of determining the orientation of CO while avoiding possible experimental error. General methodology, which can be used in other photoselection experiments determining precise angle between transition dipoles, is described.

Materials and Methods

Sperm whale myoglobin was received in solution form: *ca.* 10 mM Mb^{12}CO in D_2O buffered with 100 mM potassium phosphate, pD 7.5. To exchange ^{13}CO for ^{12}CO, the MbCO was first converted to Mb by purging with N_2 for 4 hours while illuminating the surface of the solution with 1W of visible light from an Ar^+ laser. After removal of the ^{12}CO, an equimolar concentration of freshly prepared sodium dithio-

866 *Bull. Korean Chem. Soc.* **2002**, Vol. 23, No. 6

Manho Lim

nite (Aldrich. 85%) was added to insure that all the Mb was in the reduced form and the solution was equilibrated with 1 atm ^{13}CO (Cambridge Isotope Laboratories. 99% ^{13}C, <1% ^{18}O) for 12 hours. The solution was concentrated to *ca.* 14 mM by centrifugation at 5000 g in a Centricon-10 concentrator. To remove light scattering sources such as dust particles and denatured protein aggregates. the sample was centrifuged at 5000 g for 15 min. prior to loading into gastight 100 μm path length liquid sample cell (Harrick Scientific Corporation, 2 mm-thick CaF$_2$ windows). Throughout the experiment sample concentration and validity was routinely characterized using uv-vis (Beckman. DU 600) and FTIR (Nicolet. Series 800) spectroscopy. Because water is a strong mid-IR absorber, the sample was prepared in D$_2$O with ^{13}CO ligand to isotopically shift interested spectrum into a region with greater IR transmission.

The details of the time-resolved polarized mid-IR absorption spectrometer has been described elsewhere.[31,32] Briefly. a linearly polarized pump pulse photolyzes the sample and its transient mid-IR absorbance is probed with an optically delayed, linearly polarized mid-IR probe pulse (sub-200 fs FWHM). To attain the spectral resolution needed to record the vibrational spectrum of CO. the broadband transmitted mid-IR probe pulse (250 cm^{-1} FWHM) is routed through an IR monochromator and a 3 cm^{-1} spectral slice is detected with an amplified N$_2$(*l*)-cooled InSb photodetector (EG&G). The transient spectra are obtained by tuning grating of the computer-controlled monochromator. To record the sample transmission. the signal is normalized with respect to a reference mid-IR pulse that is routed through the same monochromator and detected with a matched IR photodetector. The pump-induced change in the absorbance of the sample, Δ*A* is determined by chopping the pump pulse at half the repetition frequency of the laser and computing the difference between the pumped and unpumped absorbance.

The samples were photolyzed with 35ps. 527 nm pulses. At this wavelength. the heme is a circular absorber[33] and the relationship between polarization anisotropy and CO orientation is simplified (see next section). The pump and probe pulses were focused to ≈ 250 μm and ≈ 150 μm diameter spots. respectively. The pump spot was made significantly larger than the probe spot to ensure spatially uniform photolysis across the spatial dimensions of the probe pulse. The pump-probe optical delay was set to 100 ps. This delay is long compared to the 6 ps thermal relaxation time of the photolyzed protein[34] and the 35 ps pump pulse duration. but is short compared to the several hundred ns time for ligand escape from the docking site[35] and the rotational diffusion times of the protein. The sample cell was rotated sufficiently fast to provide a fresh sample for each photolysis pulse. The rotating sample cell was enclosed in a home-built refrigerator and maintained at 10 °C.

During a wavelength scan. the polarization of the photolysis pulse was alternated between parallel and perpendicular orientations using a computer-controlled liquid-crystal retarder (Meadowlark). This device allows us to measure both polarized spectra nearly simultaneously and afforded

greater immunity to instrumental drift. Special care was taken to ensure that both polarizations were pure (extinction ratios were routinely better than 1000 : 1) and of equal intensity.

Theory

In this section we present a brief theoretical description of the photoselection spectroscopy for dynamics and geometrical information. In particular we describe a systematic way of determining precise structural information from measured polarization anisotropy. The description is focused toward determining the CO orientation in heme proteins but it is readily generalized to determination of angles between transition dipoles of other molecules.

When an isotropic sample solution is photolyzed or photoexcited with a linearly polarized pump pulse, those molecules whose transition dipole moments happen to be oriented along the polarization direction absorb light most efficiently. thereby introducing an anisotropic distribution of photodissociated or photoexcited molecules in solution. Because of this anisotropic orientational distribution. the absorbance by the probe transition dipole of the sample will depend on whether the probe polarization is oriented parallel ($\Delta A^{\parallel}$) or perpendicular ($\Delta A^{\perp}$) to the pump polarization. The polarization anisotropy. $r(t)$ defined as $\dfrac{\Delta A^{\parallel}(t) - \Delta A^{-}(t)}{\Delta A^{\parallel}(t) + 2\,\Delta A^{-}(t)}$ is given by:

$$r(t) = 0.4 \langle P_2[\hat{\mu}_{pump}(0) \bullet \hat{\mu}_{probe}(t)] \rangle . \qquad (1)$$

where $P_2(x)$ is the second order Legendre polynomial 1/2 $(3x^2-1)$. The unit vectors $\hat{\mu}_{pump}(0)$ and $\hat{\mu}_{probe}(t)$ correspond to the transition dipole directions for the pumped transition at time zero and the probed transition at time *t* after pump. respectively. The $\langle ... \rangle$ indicates an ensemble average of molecules.

When a solution of MbCO is photolyzed at a wavelength where the heme possesses a two-fold degenerate transition dipole in its plane (at such wavelengths. the heme is called circular absorber), $r(t)$ is the average of the anisotropies for *x*- and *y*-polarized absorption. *i.e.*, $r(t) = 1/2[r_x(t) + r_y(t)] = -1/2r_z(t) = -0.2 \langle P_2[\hat{z}(0) \bullet \hat{q}(t)] \rangle$.[23] where *z* is the direction perpendicular to the heme plane and $\theta(t)$ is the angle between the C-O bond at time *t* and the heme plane normal at time zero (see Figure 1). The second equality comes from the fact that $\cos^2\alpha_{x\theta} + \cos^2\alpha_{y\theta} + \cos^2\alpha_{z\theta} = 1$. Therefore $r(t)$ is simply related to the orientation of CO according to

$$r(t) = -0.3 \langle \cos^2\theta(t) \rangle + 0.1 \qquad (2)$$

Here the angle θ spans the range $0° \leq \theta \leq 90°$. giving rise to $-0.2 \leq r(t) \leq 0.1$.

Since rotational diffusion of the protein randomizes the orientation of the photoselected hemes. the polarization anisotropy at pump-probe delay time of zero. $r(0)$ is necessary to obtain the angles between transition dipoles. $\theta(0)$ free
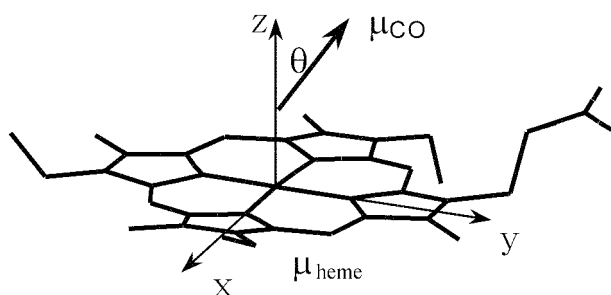
Figure 1. The hemeCO coordinate system in heme proteins. The angle between the CO bond and the heme plane normal is represented by θ. Transition dipole moment of heme, μ_{heme} lies in the plane of the heme and that of CO, μ_{CO} is along the CO bond axis.

from the contribution from the orientational dynamics. If the measurement is made at a pump-probe time delay that is much shorter than the rotational diffusion time of the protein (8 ns for Mb at 288K[36]), the measured anisotropy can be approximated to $r(0)$. Furthermore, since rotational diffusion for large molecule like Mb is well approximated with exponential decay function, the $r(0)$ is readily calculated from the measured anisotropy $r(t)$. For example, the rotational diffusion time of the MbCO sample in our experiment contributes less than a 1% reduction in the absolute value of the measured anisotropy in pump-probe delay time of 100 ps.

As the level of photolysis or photoexcitation increases, the pump-induced change in the absorbance of the sample increases, however, the absolute value of the measured anisotropy decreases. As the level of photolysis or photoexcitation approaches 100%, $\Delta A^{\parallel}$ and ΔA^{-} converge to the same value (dictated by the isotropic sample absorbance) and the anisotropy goes to zero. Clearly, a precise structural determination requires the polarization anisotropy in the limit of zero pump-induced change, r_{lim}. Practically, r_{lim} is calculated by using a correction factor that extrapolates the anisotropy measured at finite pump-induced change, r_{exp}. to that at zero pump-induced change.[19-21] Using the notation of Ansari and Szabo,[19]

$$r_{lim} = \frac{r_{exp}}{\left(\dfrac{a_2}{1-a_0}\right)} \tag{3}$$

where $a_0 = \int_0^1 \exp(-\varepsilon I_0(1 - \sigma P_2(x)))dx$ and

$a_2 = 5\int_0^1 P_2(x)\exp(-\varepsilon I_0(1 - \sigma P_2(x)))dx$

The term $(1-a_0)$ is the fraction of molecules photolyzed or photoexcited by the pump pulse and a_2 is proportional to the linear dichroism induced by linear polarized excitation of an isotropic system. I_0 is the time integral of the pump pulse intensity over the duration of that pulse, ε is the isotropic extinction coefficient at the pump wavelength, $\sigma = 1$ for a circular absorber and $\sigma = -2$ for a linear absorber.

To apply this correction, a distinction must be made between a sample that is optically *thin* versus optically *thick*. An optically thin sample is one in which the fraction of

molecules photolyzed or photoexcited remains uniform as the pump pulse passes through the sample. This requires that the absorbance of the sample be small at the pump wavelength. For an optically thin sample, the value r_{lim} can be calculated directly from the measured anisotropy using Equation 3. In case that the absolute intensity of the interested signal is small, a fairly concentrated sample is required to perform these experiments and the samples are optically thick. An optically thick sample is one in which the fraction of molecules pumped decreases as the pump pulse passes through and is absorbed by the sample.

To correct for finite pump-induced change of an optically thick sample, we imagine the sample cell to be divided into a large number of optically thin slices along the path of the pump pulse. Then the polarization anisotropy within each slice i would be

$$r_i = \frac{\Delta A_i^{\parallel} - \Delta A_i^{\perp}}{3\Delta A_i^{M}} \tag{4}$$

where $\Delta A_i^{M} = 1/3(\Delta A^{\parallel} - 2\Delta A^{\perp})$ is the pump-induced change in the isotropic absorbance measured at the so-called "magic" angle of $54.74°$. Because absorbances are additive, the absorbance of an optically thick sample is the sum of absorbances over all slices. i.e.. $\Delta A = \Sigma \, \Delta A_i$. Therefore, the measured polarization anisotropy can be rewritten as

$$r_{exp} = \frac{\sum_i \Delta A_i^{\parallel} - \sum_i \Delta A_i^{\perp}}{3\Delta A^{M}}$$

$$= \sum_i \left(\frac{\Delta A_i^{\parallel} - \Delta A_i^{-}}{3\Delta A_i^{M}} \times \frac{\Delta A_i^{M}}{\Delta A^{M}}\right)$$

$$= \sum_i r_i f_i \tag{5}$$

where $f_i = \Delta A_i^{M}/\Delta A^{M}$ is the fraction of the pump-induced population that resides in slice i. Hence, the anisotropies in each optically thin slice of the sample can be summed in a population-weighted fashion to recover the anisotropy measured in an optically thick sample.

By extension, the polarization anisotropy in the limit of zero pump-induced change can be determined by dividing the measured anisotropy by a sum of population weighted correction factors. To calculate the appropriate correction factor, we first rearrange Equation 3 to solve for the polarization anisotropy in slice i.

$$r_i = r_{lim}\left(\frac{a_2}{1-a_0}\right)_i \tag{6}$$

where a_0 and a_2 must be evaluated for the degree of pump-induced change within slice i. Because r_{lim} is independent of the level of pump-induced change, it doesn't require an index. As shown earlier, the measured anisotropy in an optically thick sample is the population-weighted sum over all slices.

$$r_{exp} = \sum_i r_i f_i = r_{lim} \sum_i \left(\frac{a_2}{1-a_0}\right)_i f_i \tag{7}$$

Consequently.

$$r_{lim} = \frac{r_{exp}}{\sum_i \left(\frac{a_2}{1 - a_0}\right)_i f_i} \tag{8}$$

and the appropriate correction factor becomes the population-weighted sum of correction factors for each slice i. Determining the anisotropy that would be measured in the limit of zero pump induced change with an optically thick sample, therefore, requires that the degree of pump induced change be determined as a function of path length through the sample.

The degree of pump induced change within each optically thin slice of the sample can be calculated given the absorbance of the sample at the pump wavelength (A), the absorbance of a pump induced sample at the same wavelength (A^*), and the average degree of pump induced change. The absorbance of the pump induced sample, A^*, is required because its absorbance affects the penetration of the pump pulse.

Results and Discussion

For the distinction between an optically thin and thick sample, the gradient in the fraction of pump-induced molecules along the depth of the sample is calculated for pump absorbance of 1 with an average pump-induced change of 10%, 20%, and 30% and A^*/A of 0, 1, 2. As shown in Figure 2(a), the gradient is significant even for 10% bleach of the sample, and gets more significant as the average pump-induced change or the ratio of A^*/A increase. The MbCO sample with the absorbance of 1.4 at 527 nm was used to attain the signal-to-noise ratio needed to make a definitive determination of the CO orientation. The profile of the photolyzed population for this sample across the depth of the sample is also calculated and shown in Figure 2(b). Under the experimental conditions employed in this study an average photolysis of 10% (20%) lead to 30% (54%) photolysis at the front of the sample and only 1.5% (3.3%) at the rear of the sample.

The correction factor, $\sum_i (a_2/(1 - a_0))_i f_i$, is plotted as a function of the absorbance, A with three levels of pump induced change and three ratios of A^*/A. As shown in Figure 3, the correction factor at higher levels of pump induced change becomes a strong function of A and A^*, causing the optically thick correction factor to differ substantially from the optically thin limit. For typical experimental conditions in determining the CO orientation of heme proteins. *e.g.*, $A =$ 1.5, $A^*/A = 1$, and average photolysis of 20%, the extent of correction for an optically thick sample is nearly 2 times that which would be predicted for an optically thin sample. Clearly, these simulations show that a precise structural determination requires the correction factor for optically thick sample.

In previous section we showed that the polarization anisotropy measured in an optically thick sample is simply the population-weighted sum of anisotropies that would be
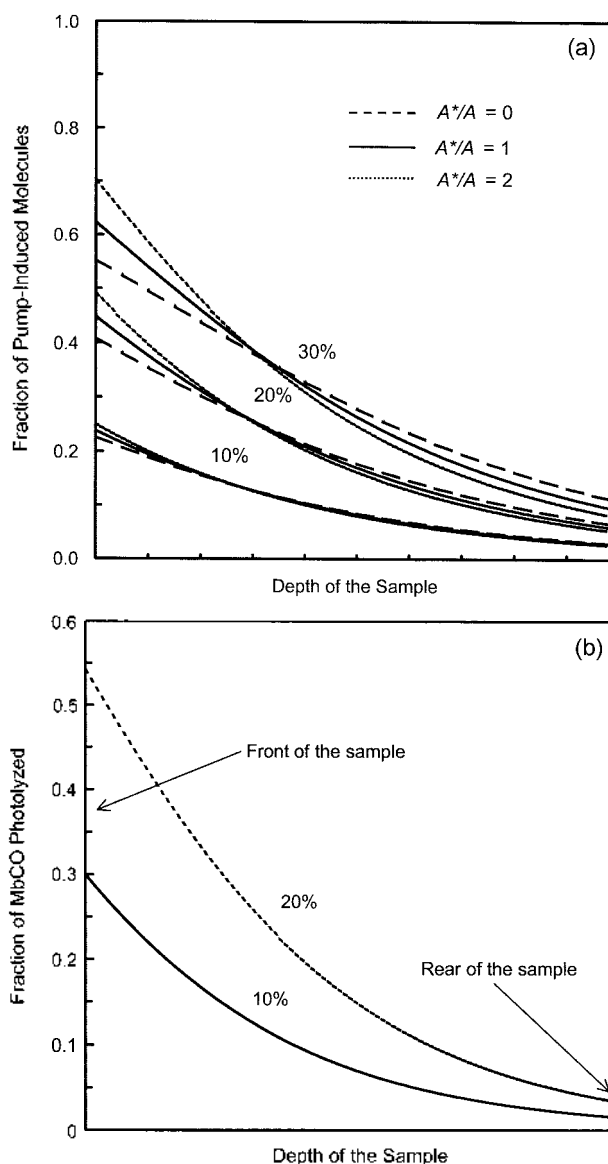

Figure 2. (a) The gradient in the fraction of pump-induced molecules along the depth of the sample with sample absorbance A = 1 at the pump wavelength. The gradient is shown for average pump-induced change of 10%, 20%, and 30%. For each degree of pump-induced change, the depth profile is shown for A^*/A = 0, 1, and 2 as dashed, solid, and dotted lines, respectively. (b) The calculated photolysis profile for the MbCO sample used in this study. The parameters used in the calculation are A = 1.4, A^*/A = 0.798 and average photolysis of 10% (solid line) and 20% (dotted line).

measured if the sample were divided into a large number of optically thin slices. To validate the derivation experimentally, the polarization anisotropy of MbCO for various extent of fractional photolysis was measured and is shown in Figure 4. As the level of photolysis increases, the absolute value of the polarization anisotropy decreases monotonically. The experimental values are well described by the solid line, the polarization anisotropy corrected for finite photolysis of an optically thick sample, which represents the best-fit curve calculated using the approach outlined in section III. Experi-
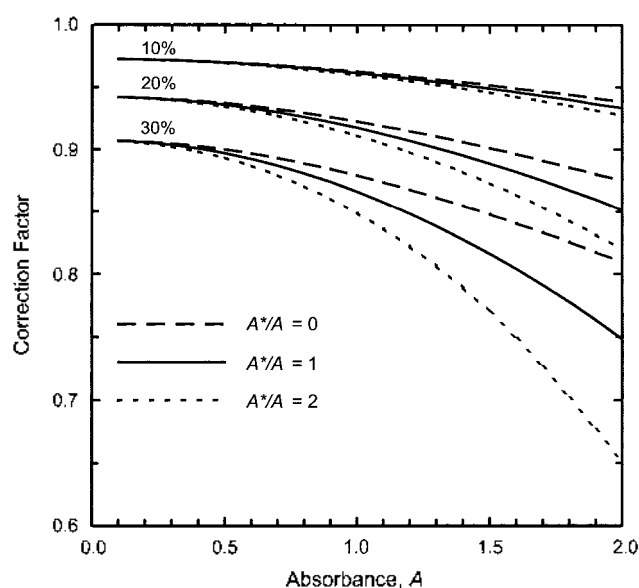
Figure 3. The correction factor for finite photolysis of an optically thick sample is plotted versus sample absorbance (A) at the photolysis wavelength. The correction factor is shown for 10%, 20%, and 30% photolysis on the average. For each degree of photolysis, the correction factor is shown for A^*/A = 0, 1, and 2 as dashed, solid, and dotted lines, respectively. To determine r_{lim}, the polarization anisotropy that would be measured in the limit of zero photolysis, r_{exp}, the experimentally measured anisotropy, must be divided by the correction factor calculated using equation 8.

Figure 4. Polarization anisotropy measured as a function of the average level of photolysis within an optically thick sample. The filled circles correspond to the anisotropy measured for Mb^{13}CO : D$_2$O at 2.2%, 3.4%, 5.6%, 9.3%, 10.6%, 13.0%, and 16.3% photolysis on the average. The error bars correspond to one standard deviation. The thick line corresponds to the predicted polarization anisotropy given our optically *thick* sample. The zero-photolysis limit is r_{lim} = -0.192. The thin line represents the polarization anisotropy expected when measured in an optically *thin* sample (see text for details).

mentally determined absorbances with A = 1.4 and A^*/A = 0.789 were used to fit the data and to obtain r_{lim} = -0.192. The dashed line represents the anisotropy as a function of fraction photolysis that is predicted for an optically thin sample if the experimentally determined r = -0.176.[19,21] the polarization anisotropy at 20% photolysis when r_{lim} = -0.192. The correction factor required for an optically *thick* sample is greater than that required for an optically *thin* sample at all levels of photolysis, but is most severe at high levels of photolysis. Correcting the measured anisotropy at 20% photolysis assuming optically thin sample, one would predict that r_{lim} = -0.183 as opposed to the actual value r_{lim} = -0.192. If the effect of an optically thick sample is ignored, the absolute value of the anisotropy is underestimated, thereby influencing significantly the orientation calculated for CO. These results experimentally validate the theoretical extrapolation to zero photolysis in optically thick samples, allowing us to only measure the polarization anisotropy at one level of photolysis for a precise structural determination of CO orientation in heme proteins.

In addition to considering the gradient in photolysis through an optically thick sample, we also considered the gradient in photolysis across the spatial profile of the probe spot. When the focused pump pulse is not sufficiently large compared to the focused probe pulse, a gradient in photolysis appears across the spatial profile of the probe pulse, affecting the determination of r_{lim}. We performed our experiments with two different ratios of pump/probe spot sizes: 1.7 and 2.7. Within experimental error, the anisotropy measured with the
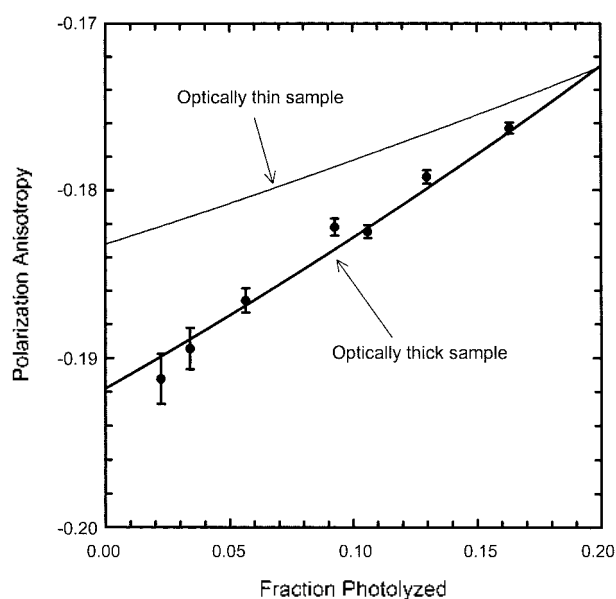
two different spot sizes was the same, suggesting that a ratio of 1.7 is sufficient to minimize the effects of a spatial gradient in photolysis. Apparently in our experimental conditions, where the ratio of 1.7 was employed, the fractional photolysis across spatial profile of the probed spot was sufficiently uniform that additional corrections were unnecessary. As the ratio of pump/probe spot size decreases, the gradient in photolysis across the spatial profile of the probe pulse would be getting more significant, requiring a spatial correction.

Time-resolved polarized mid-IR absorbance spectra of photolyzed MbCO is shown in Figure 5. The spectra retrace the equilibrium IR spectra of MbCO and correspond to the photolysis-induced depletion of bound CO. The left ordinate represents the pump-induced change in the absorbance of the sample. The right ordinate represents the polarization anisotropy extrapolated to the limit of zero photolysis, r_{lim}. The spectra reveal two features, a main band and a shoulder. It had been suggested that multiple bands arise from multiple conformations of the protein, each of which can have a different CO orientation.[5,24] However, the polarization anisotropy is virtually constant across the spectra, meaning θ must be constant as well.[15]

According to Equation (2), r_{lim} is related to the ensemble average. Since thermal motion of CO and its surroundings at 283 K ensures that the angular distribution of CO is distributed about some equilibrium orientation, a definitive determination of the CO orientation requires knowledge of the orientational probability distribution function. If one
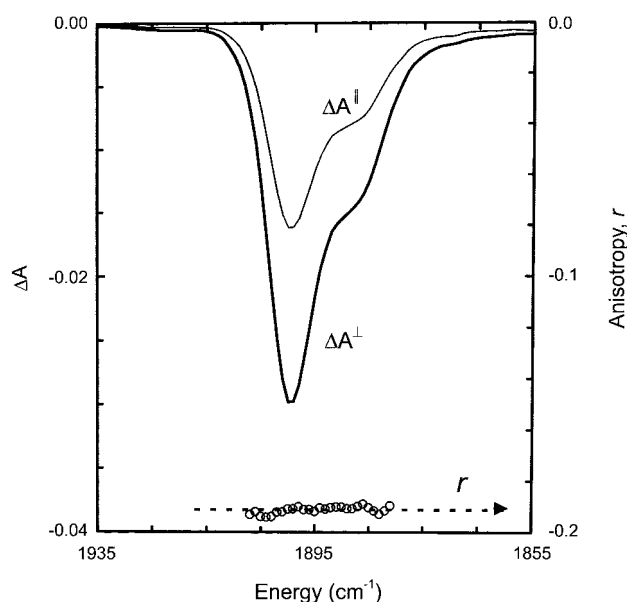
Figure 5. Time-resolved mid-IR absorbance spectra of photolyzed $Mb^{13}CO : D_2O$ at 283 K. The spectra were obtained with the pump pulse polarized perpendicular, $\Delta A^{\perp}$ (thick line) and parallel, $\Delta A^{\parallel}$ (thin line) to the probe pulse. The polarization anisotropy (open circles) corresponds to the anisotropy in the zero-photolysis limit (see text for details). The dashed horizontal line points to the population-weighted average of the anisotropy across the spectra.

assumes a sharply peaked distribution of angles θ, *i.e.*, a delta function for angular distribution function, the orientation of CO corresponding to $r_{lim} = -0.192$ is $9.5°$. The broader the distribution in θ, the smaller the absolute value of the measured anisotropy, even if the equilibrium orientation remains unchanged. Therefore, $9.5°$ represents an *upper limit* for the equilibrium orientation of bound CO. We estimated an orientational probability distribution function for bound CO from the force constant of the axial Fe-C-O tilting mode and obtained $\theta = 7.4°$.[15]

The equilibrium orientation of bound CO obtained after correcting for the orientational distribution is still an upper limit. Thermal motion of the heme and its surroundings causes the heme to deviate from planarity, thereby giving rise to a nonzero transition moment along the direction of the heme normal. Moreover, the heme can librate within the protein on a time scale that is fast compared to the 100 ps time delay of our measurement.[37] Because the CO is connected to the heme, motion of the heme should translate into motion of the CO. This motion causes a time-dependent decay of the measured anisotropy, the magnitude of which is determined by the amplitude of the heme librational motion. Furthermore, the Fe-C-O bending motion at 283 K spans $\pm 4.5°$,[32] a range larger than our absolute uncertainty in the CO orientation. All factors mentioned above that influence the polarization anisotropy tend to reduce its absolute value. The corrections that we have made, plus those we have not, demonstrate that the orientation of CO may be as small as $0°$ from the heme plane normal.[15]

In conclusion, a definitive determination of the equilibrium orientation of CO in heme proteins requires the polarization

anisotropy in the limit of zero photolysis at pump-probe delay time of zero and the orientational distribution function of CO. In extrapolating the measured polarization anisotropy to that in the limit of zero photolysis, correction for finite photolysis of an optically thick sample is significant. However, the method to account for the correction factor for finite photolysis of an optically thick sample has not been developed in earlier experiments. Their determinations either neglected fractional photolysis effects or corrected for them incompletely. Here we have presented a way of getting the correction factor for finite photolysis of an optically thick sample, thereby establishing the ground for a precise determination of CO orientation in heme proteins. This method can be readily applied to acquire the correction factor for finite pump-induced change in other photoselection experiments determining precise angle between transition dipoles.

References

1. Springer, B. A.; Sligar, S. G.; Olson, J. S.; Phillips, G. N., Jr. *Chem. Rev.* **1994**, *94*, 699.
2. Collman, J. P.; Brauman, J. I.; Halbert, T. R.; Suslick, K. S. *Proc. Natl. Acad. Sci. U. S. A.* **1976**, *73*, 3333.
3. Antonini, E.; Brunori, M. *Hemoglobin and Myoglobin in Their Reactions with Ligands*; North-Holland Publishing Company: London. 1971.
4. Coburn, R. F. *Am. N. Y. Acad. Sci.* **1970**, *174*, 11.
5. Kuriyan, J.; Wilz, S.; Karplus, M.; Petsko, G. A. *J. Mol. Biol.* **1986**, *192*, 133.
6. Peng, S. M.; Ibers, J. A. *J. Am. Chem. Soc.* **1976**, *98*, 8032.
7. Collman, J. P.; Gagne, R. R.; Reed, C. A.; Robinson, W. T.; Rodley, G. A. *Proc. Natl. Acad. Sci. U. S. A.* **1974**, *71*, 1326.
8. Jameson, G. B.; Rodley, G. A.; Robinson, W. T.; Gagne, R. R.; Reed, C. A.; Collman, J. P. *Inorg. Chem.* **1978**, *17*, 850.
9. Jameson, G. B.; Molinaro, F. S.; Ibers, J. A.; Collman, J. P.; Brauman, J. I.; Rose, E.; Suslick, K. S. *J. Am. Chem. Soc.* **1980**, *102*, 3224.
10. Phillips, S. E. V. *J. Mol. Biol.* **1980**, *142*, 531.
11. Caughey, W. S. *Am. N. Y. Acad. Sci.* **1970**, *174*, 148.
12. Stryer, L. *Biochemistry*; W. H. Freeman and company: San Francisco, 1988.
13. Ray, G. B.; Li, X.-Y.; Ibers, J. A.; Sessler, J. L.; Spiro, T. G. *J. Am. Chem. Soc.* **1994**, *116*, 162.
14. Hu, S.; Vogel, K. M.; Spiro, T. G. *J. Am. Chem. Soc.* **1994**, *116*, 11187.
15. Lim, M.; Jackson, T. A.; Anfinrud, P. A. *Science* **1995**, *269*, 962.
16. Kachalova, G. S.; Popov, A. N.; Bartunik, H. D. *Science* **1999**, *284*, 473.
17. Spiro, T. G.; Kozlowski, P. M. *Acc. Chem. Res.* **2001**, *34*, 137.
18. Albrecht, A. C. *J. Mol. Spec.* **1961**, *6*, 84.
19. Ansari, A.; Szabo, A. *Biophys. J.* **1993**, *64*, 838.
20. Ivanov, D.; Sage, J. T.; Keim, M.; Powell, J. R.; Asher, S. A.; Champion, P. M. *J. Am. Chem. Soc.* **1994**, *116*, 4139.
21. Hansen, P. A.; Moore, J. N.; Hochstrasser, R. M. *Chem. Phys.* **1989**, *131*, 49.
22. Moore, J. N.; Hansen, P. A.; Hochstrasser, R. M. *Chem. Phys. Lett.* **1987**, *138*, 110.
23. Moore, J. N.; Hansen, P. A.; Hochstrasser, R. M. *Proc. Natl. Acad. Sci. U. S. A.* **1988**, *85*, 5062.
24. Ormos, P.; Braunstein, D.; Frauenfelder, H.; Hong, M. K.; Lin. S.

L.: Sauke, T. B.; Young, R. D. *Proc. Natl. Acad. Sci. U. S. A.* **1988**. *85*, 8492.

25. Locke, B.; Lian, T.; Hochstrasser, R. M. *Chem. Phys.* **1991**, *158*, 409.

26. Rothberg, L. J.; Roberson, M.; Jedju, T. M. *Proc. SPIE-Int. Soc. Opt. Eng.* **1991**, *1599*, 309.

27. Braunstein, D. P.; Chu, K.; Egeberg, K. D.; Frauenfelder, H.; Mourant, J. R.; Nienhaus, G. U.; Ormos, P.; Sligar, S. G.; Springer, B. A.; Young, R. D. *Biophys. J.* **1993**, *65*, 2447.

28. Lian, T.; Locke, B.; Kitagawa, T.; Nagai, M.; Hochstrasser, R. M. *Biochemistry* **1993**, *32*, 5809.

29. Locke, B.; Lian, T.; Hochstrasser, R. M. *Chem. Phys.* **1995**, *190*, 155.

30. McMahon, M. T.; deDios, A. C.; Godbout, N.; Salzmann, R.; Laws, D. D.; Le, H.; Havlin, R. H.; Oldfield, E. *J. Am. Chem. Soc.* **1998**, *120*, 4784.

31. Anfinrud, P. A.; Lim, M.; Jackson, T. A. *Proc. SPIE-Int. Soc. Opt. Eng.* **1994**, *2138*, 107.

32. Lim, M.; Jackson, T. A.; Anfinrud, P. A. *J. Chem. Phys.* **1995**, *102*, 4355.

33. Eaton, W. A.; Hofrichter, J. *Methods Enzymol.* **1981**, *76*, 175.

34. Lim, M.; Jackson, T. A.; Anfinrud, P. A. *J. Phys. Chem.* **1996**, *100*, 12043.

35. Lim, M.; Jackson, T. A.; Anfinrud, P. A. *unpublished material*.

36. Albani, J.; Alpert, B. *Chem. Phys. Lett.* **1986**, *131*, 147.

37. Henry, E. R. *Biophys. J.* **1993**, *64*, 869.